Reduced calcification and lack of acclimatization by coral colonies growing in areas of persistent natural acidification

Elizabeth D. Crook[a], Anne L. Cohen[b], Mario Rebolledo-Vieyra[c], Laura Hernandez[c], and Adina Paytan[a,1]

[a]Institute of Marine Sciences, University of California, Santa Cruz, CA 95064; [b]Department of Marine Geology and Geophysics, Woods Hole Oceanographic Institution, Woods Hole, MA 02543; and [c]Unidad de Ciencias del Agua, Centro de Investigación Científica de Yucatán, Cancún, Quintana Roo, Mexico, 77524

Edited by David M. Karl, University of Hawaii, Honolulu, HI, and approved May 23, 2013 (received for review January 28, 2013)

As the surface ocean equilibrates with rising atmospheric CO_2, the pH of surface seawater is decreasing with potentially negative impacts on coral calcification. A critical question is whether corals will be able to adapt or acclimate to these changes in seawater chemistry. We use high precision CT scanning of skeletal cores of *Porites astreoides*, an important Caribbean reef-building coral, to show that calcification rates decrease significantly along a natural gradient in pH and aragonite saturation (Ω_{arag}). This decrease is accompanied by an increase in skeletal erosion and predation by boring organisms. The degree of sensitivity to reduced Ω_{arag} measured on our field corals is consistent with that exhibited by the same species in laboratory CO_2 manipulation experiments. We conclude that the *Porites* corals at our field site were not able to acclimatize enough to prevent the impacts of local ocean acidification on their skeletal growth and development, despite spending their entire lifespan in low pH, low Ω_{arag} seawater.

reef framework | caribbean corals acidic springs

Scleractinian corals, whose calcium carbonate ($CaCO_3$) skeletons provide the structural framework of coral reef ecosystems, are subject to numerous direct and indirect stressors and are facing steep global decline (1–3). As the ocean absorbs anthropogenic CO_2, surface ocean pH and the availability of carbonate ions to corals and other reef calcifiers are decreasing (1–5). Global climate models predict a drop of 0.3 pH units, from 8.1 to 7.8 by the end of the 21st century (6–8), resulting in a 50% reduction in carbonate ion concentration (9). Consequently, it is predicted that ocean acidification will result in a widespread reduction in coral calcification by the year 2065 (10), causing large-scale reef degradation and loss (11).

The predicted response of coral reef calcification to decreasing aragonite-saturation (Ω_{arag}) state is based primarily on model calculations of future Ω_{arag} (6, 7, 9, 12) and the observed response of coral calcification to low Ω_{arag} in short-term laboratory-based or mesocosm carbonate chemistry manipulation experiments (11, 13–16). Additionally, field-based observations of net coral reef ecosystem calcification responses to changes in Ω_{arag} state in situ also suggest declines in calcification (17–21). However, key questions remain regarding the acclimation and adaptation potential of coral calcification to ocean acidification. Acclimatization, or the potential for an organism to adjust to changes in an environment via physical modifications, is distinguished from adaptation, or permanent evolutionary modifications made by an organism in response to repeated stressors. Specifically, an outstanding question is whether corals will be able to acclimate or adapt to maintain sufficient rates of calcification to sustain the reef structure (17, 22, 23). To address these questions, field-based studies where corals have been naturally exposed to chronic low pH conditions for extended periods could provide important new insights. In this study, we quantify calcification rates of the common Atlantic coral, *Porites astreoides*, growing in an environment of low pH and Ω_{arag} along the Caribbean coast of the Yucatan Peninsula, Mexico for time scales long enough for acclimation. We compare annual calcification rates of these corals with corals of the same species living in close proximity (less than 10 m away) under ambient pH and Ω_{arag} conditions. Results from short-term laboratory CO_2 manipulation experiments with the same species provide an empirical framework within which to interpret the field data, enabling us to determine whether these corals, which have been exposed to low Ω_{arag} for their entire life span, have acclimated to ocean acidification.

The karstic region of the Yucatan Peninsula is an area where low pH groundwater and seawater have been interacting since the last deglaciation ~18,000 y ago (24). Due to the high porosity of the limestone bedrock, there is no surficial runoff; rather, rainfall rapidly infiltrates the water table and is drained through a series of interconnected caves and fractures directly to the coast (25) discharging at highly localized submarine springs in close proximity to the Mesoamerican Barrier Reef. Before the water is discharged, extensive mixing with seawater occurs within the aquifer. As a result, water with low pH, high dissolved inorganic carbon (DIC), high alkalinity, low Ω_{arag}, and near oceanic salinities is discharged at submarine springs (Table S1, Fig. S1, and refs. 25–27). Light, temperature, and sedimentation conditions are similar between the springs and control sites although nutrient levels are higher at the springs (26).

Importantly, the discharge at these springs has been continuous for millennia: thus, the coral colonies at these sites settled, calcified, and grew into mature colonies within the plume of low-pH groundwater discharge. The Yucatan springs represent areas where the ecosystem has had ample time to acclimate to low-pH conditions. Previous work off the coast of Puerto Morelos, Quintana Roo, Mexico, demonstrates that these springs, despite their low Ω_{arag} water, are host to corals and other benthic calcifiers, although coral diversity and coral cover are reduced close to the springs, likely driven by the chronically low Ω_{arag} conditions (26). Monitoring over a 3-y period indicates that the pH of the discharging water fluctuates considerably on multiple time scales, but the water at the center of the springs remains undersaturated for a majority of the time (26, 28). To compliment previous findings at Puerto Morelos, we measured calcification rates of the corals found in close proximity to four springs characterized by low saturation and near oceanic salinities (>30, ~93% of the time, Fig. S1) and compared them to similar colonies found nearby in ambient seawater conditions.

Results

Skeletal samples from 14 *P. astreoides* colonies were obtained from the vicinity of four springs at Puerto Morelos: 7 within the

Author contributions: E.D.C. and A.P. designed research; E.D.C., A.L.C., M.R.-V., L.H., and A.P. performed research; A.L.C., M.R.-V., L.H., and A.P. contributed new reagents/analytic tools; E.D.C., A.L.C., and A.P. analyzed data; and E.D.C., A.L.C., and A.P. wrote the paper.

The authors declare no conflict of interest.

This article is a PNAS Direct Submission.

[1]To whom correspondence should be addressed. E-mail: apaytan@ucsc.edu.

This article contains supporting information online at www.pnas.org/lookup/suppl/doi:10.1073/pnas.1301589110/-/DCSupplemental.

Downloaded from https://www.pnas.org by 124.148.102.239 on April 12, 2022 from IP address 124.148.102.239.

impact of the discharge ($\Omega_{arag} < 2.0$), and 7 from areas with ambient seawater conditions ($\Omega_{arag} > 3.5$) in close proximity to the springs (less than 10 m away). Cores were removed using a handheld drill fitted with a 1-inch round diamond tipped coring bit. Dried, intact cores were scanned using a Siemens Volume Zoom Spiral Computerized Tomography (CT) scanner at the Woods Hole Oceanographic Institution (29, 30) together with a set of pristine coral standards the densities of which were determined independently by weight and volume calculations, to enable precise quantification of annual linear extension rates ($cm{\cdot}y^{-1}$), density ($g{\cdot}cm^{-3}$), and calcification ($g{\cdot}cm^{-2}{\cdot}y^{-1}$) (Fig. 1). The 3D images produced from the CT scans were also used to assess the extent of erosion in each core. After CT scanning, each core was sliced in half using a high precision wet saw fitted with a diamond wafer blade. Tissue thickness, a measure of the volume of coral soft tissue occupying the skeleton, was measured on each core half using a Nikon SMZ1500 stereo microscope and SPOT imaging software. We define tissue thickness as the distance between the last (most recently accreted) dissepiment and the tip of the calical walls. At the time of coring, in situ temperature and pH were measured and water samples were taken for DIC, total alkalinity (TA), calcium and nutrient concentrations, and salinity. Chemical measurements taken at the time of sampling, as well as during previous sampling events (26, 28), indicate that all coral skeletal cores taken directly from the springs were residing in undersaturated ($\Omega_{arag} < 1$) or mildly supersaturated water ($1 < \Omega_{arag} < 2$). The remaining cores were removed from corals residing in ambient seawater coinciding with saturation states greater than 3.5.

Linear extension rates were not statistically different between corals in low pH water ($\Omega_{arag} < 2$) and corals in the ambient seawater ($\Omega_{arag} > 3.5$) ($P = 0.33$, Fig. 2*A*); however, a trend toward lower extension rates for the corals in undersaturated waters is observed ($\Omega_{arag} < 1$) (Fig. 2*B*). When divided into three saturation groups, average annual extension for each group was $0.19\ cm{\cdot}y^{-1} \pm 0.07$ ($\Omega_{arag} < 1$), $0.29\ cm{\cdot}y^{-1} \pm 0.09$ ($1 < \Omega_{arag} < 2$), and $0.30\ cm{\cdot}y^{-1} \pm 0.12$ ($\Omega_{arag} > 3.5$). The linear extension decline of 38% between ambient Ω_{arag} and undersaturation may indicate a threshold response (Fig. 2*B*), although the trend between ambient and undersaturated extension rates is not significant and more samples are required to test this hypothesis (ANOVA, $F(2,11) = 1.90$, $P = 0.19$).

Conversely, a statistically significant drop in skeletal density occurred between corals growing in ambient conditions ($\Omega_{arag} > 3.5$) and corals growing in low Ω_{arag} and undersaturated waters ($\Omega_{arag} < 2$) (ANOVA, $F(2,11) = 25.751$, $P = 0.0001$, Fig. 2*C*). Average skeletal density dropped by ~28% from $\Omega_{arag} > 3.5$ to $\Omega_{arag} < 2$. However, a Tukey HSD (Honestly Significant Difference) post hoc test reveals that the low ($1 < \Omega_{arag} < 2$) and undersaturated ($\Omega_{arag} < 1$) groups both differ significantly from the control ($P = 0.0001$) but not from each other ($P = 0.26$, Fig. 2*D*). Rather, the sharp decline in density occurred between $2.0 < \Omega_{arag} < 3.5$. Linear regression to see how Ω_{arag} predicts density shows a slope of 0.16, which is highly significantly different from zero ($P < 0.0001$), and suggests that each 1-unit decrease in Ω_{arag} is associated with a 0.16-unit decrease in density.

Annual calcification is the amount of calcium carbonate produced by each colony per year and is calculated as the product of annual extension and density. Annual calcification of *P. astreoides* declined significantly between the control ($\Omega_{arag} > 3.5$) and low saturation colonies ($\Omega_{arag} < 1$; $1 < \Omega_{arag} < 2$) (ANOVA, $F(2,11) = 7.757$, $P = 0.008$, Fig. 2*E*). Further analysis reveals that the average calcification for the undersaturated group ($0.20\ g{\cdot}cm^{-2}{\cdot}y^{-1}$) differs significantly from both the control colonies ($0.48\ g{\cdot}cm^{-2}{\cdot}y^{-1}$, $P = 0.009$) and the low saturation group ($0.35\ g{\cdot}cm^{-2}{\cdot}y^{-1}$, $P = 0.05$, Fig. 2*D*). Linear regression to see how omega predicts annual calcification shows a slope of 0.07, which is highly significantly different from zero ($P = 0.003$), and suggests that each 1-unit decrease in Ω_{arag} is associated with a 0.07-unit decrease in calcification. This translates to an approximate 30% decline in calcification from ambient conditions by the time $\Omega_{arag} = 2$, and up to a 66% decline in calcification between ambient and $\Omega_{arag} < 1$ (Fig. 2*F*). As linear extension rates did not vary significantly between low Ω_{arag} and ambient Ω_{arag} waters, the calculated decrease in calcification is driven primarily by the decrease in skeletal density with decreasing Ω_{arag}. However, the drop in calcification rate between corals living in low and undersaturated seawater was driven by the combined effect of reduced linear extension and low skeletal density. By the time undersaturation is reached, the paucity of carbonate ions for skeleton building impacts both skeletal growth parameters: upward linear extension and skeletal thickening.

Discussion

One of the challenges posed by in situ field studies is that multiple environmental parameters may covary, making it difficult to resolve the influence of Ω_{arag} on calcification from that of other factors or to assess the extent to which the influence of Ω_{arag} may be modulated by other, covarying factors. We can address this

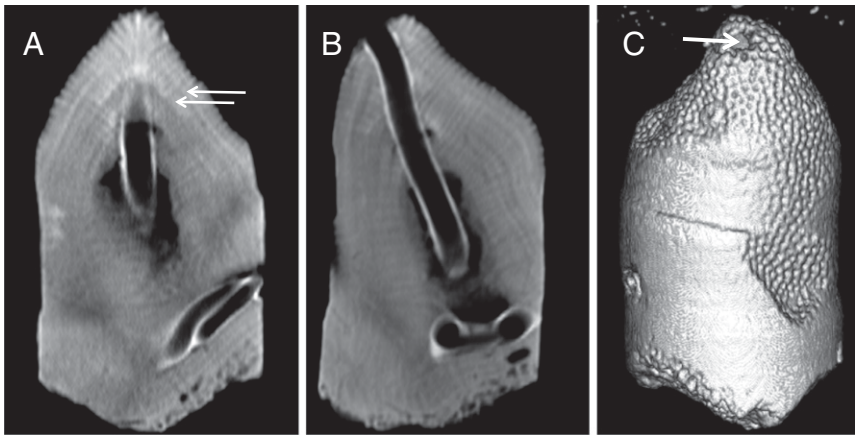

Fig. 1. CT scanned images of a core. Comparisons of linear extension (*A*) can be made to 0.5-mm accuracy by measuring the distance between high density bands (white arrows), and density can be determined at a given point via the use of coral standards. CT scanning allows for the rotation of the images (*B*) to reveal additional features in the core, including the exact dimensions of boring and erosion. The reconstructed core (*C*) reveals only a small bore hole (white arrow) that actually runs the length of the core.

Downloaded from https://www.pnas.org by 124.148.102.239 on April 12, 2022 from IP address 124.148.102.239.

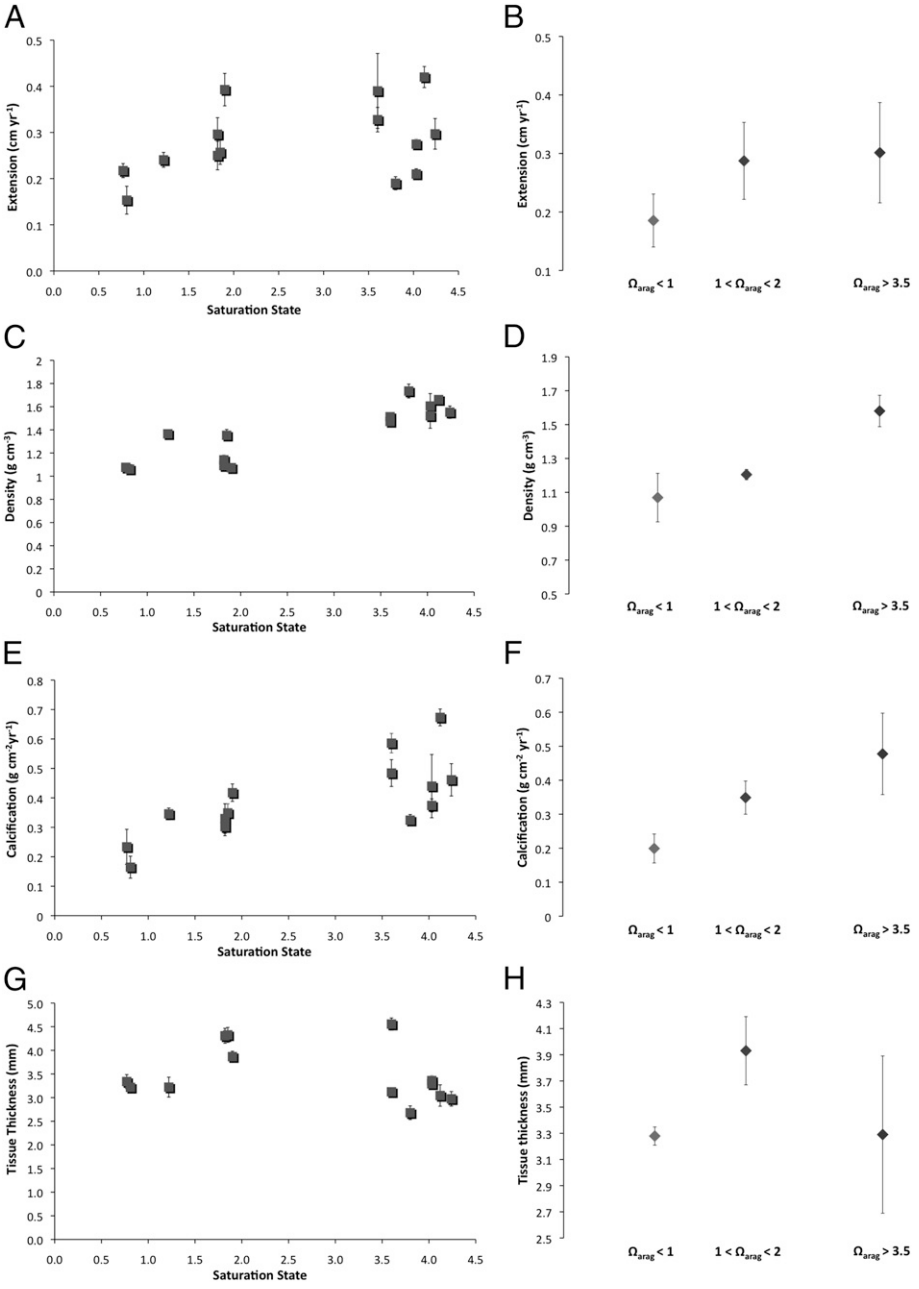

Fig. 2. Linear extension (*A* and *B*), density (*C* and *D*), calcification (*E* and *F*), and tissue thickness (*G* and *H*) as a function of saturation state for all data (*A*, *C*, *E*, and *G*) and grouped by saturation state (*B*, *D*, *F*, and *H*). In *A*, *C*, *E*, and *G*, error bars represent SE and in *B*, *D*, *F*, and *H*, error bars depict SD. No significant differences in extension ($cm \cdot y^{-1}$) are seen with decreasing saturation state ($P = 0.33$). However, a trend is noted in which extension rate drops as undersaturation is reached. Regression analysis indicates density ($g \cdot cm^{-3}$), decreasing significantly with decreasing saturation ($P < 0.0001$), by up to 28% from ambient. Calcification ($g \cdot cm^{-2} \cdot y^{-1}$) decreases by up to 66% by the time undersaturated waters are reached ($P = 0.003$). Tissue thickness does not vary significantly with saturation (*G*); however, a trend is seen where tissue thickness increases slightly where $1 < \Omega < 2$ (*H*).

question by comparing the change in *P. astreoides* calcification measured at our Yucatan study site with that observed in laboratory CO_2 manipulation experiments. In these experiments only pH and Ω_{arag} vary, whereas other environmental parameters (e.g., temperature, salinity, light) are kept constant, thus allowing us to isolate the effect of ocean acidification on *P. astreoides* calcification from other factors.

By far the majority of laboratory CO_2 manipulation experiments conducted to date show that *P. astreoides* calcification is sensitive to ocean acidification, consistent with our results from the Yucatan. Results from different experiments are consistent, showing a decline of ~40% with a 65% drop in Ω_{arag} (Fig. 3). At our Yucatan field site, the sensitivity of *P. astreoides* calcification is identical to results obtained in controlled laboratory experiments using the same species from the Atlantic or Caribbean across the same range in Ω_{arag} (31, 32). The strong agreement between field and experimental data indicates that *P. astreoides* calcification is responding to the natural Ω_{arag} gradient at the Yucatan, and not to other factors.

Global climate models predict that by the year 2100, tropical surface oceans may have a Ω_{arag} of ~2.5 (9); therefore, our study implies that net $CaCO_3$ production in Atlantic reefs on which *P. astreoides* is a major reef builder (such as Bermuda, the Virgin

Downloaded from https://www.pnas.org by 124.148.102.239 on April 12, 2022 from IP address 124.148.102.239.

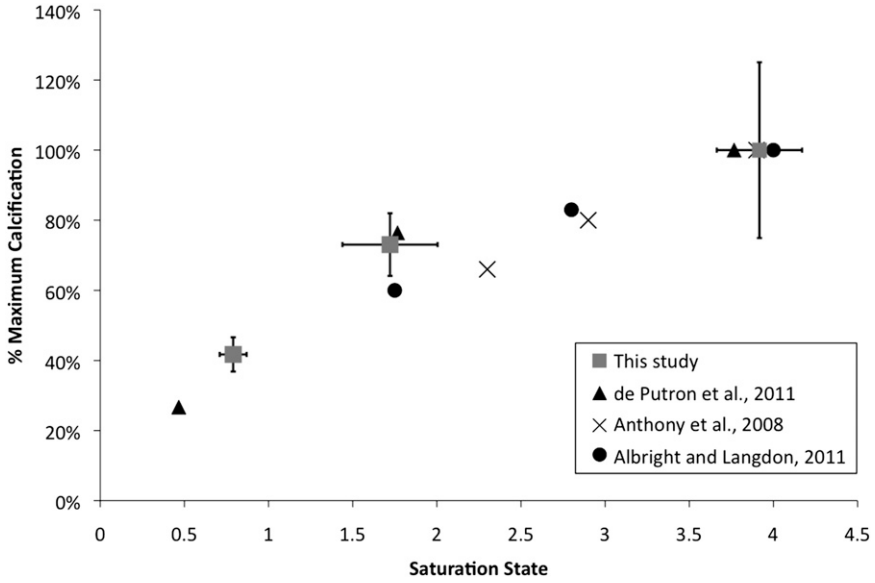

Fig. 3. Impact of Ω_{arag} on *P. astreoides* calcification in this study (squares) plotted against laboratory studies of *Porites* spp. (31–33), and *P. astreoides* in particular (31, 32). Calcification at a given saturation was calculated as a percent of the maximum observed calcification rate for each study. Error bars (this study) depict ± SD.

Islands, or Belize), could decrease significantly within the next century. The greatest decrease in calcification we observed in undersaturated ($\Omega_{arag} < 1$) waters was 66% from present day values. Using our linear regression model, we predict that *Porites* calcification could decrease by ∼15% from preindustrial values by the time tropical surface oceans reach Ω_{arag} ∼3.1 in the year 2065 (34). If atmospheric CO_2 concentrations triple (Ω_{arag} ∼2), a loss of ∼31% could result. This estimate is in line with field, mesocosm, and laboratory studies that indicate a decline in calcification between 13% and 22% (31, 35–38). When combined with the negative impacts of other stressors, including rising sea surface temperatures that cause mass bleaching (2), pollution, and overfishing, ocean acidification is likely to deal a significant blow to the health of Atlantic coral reefs within the next few decades (1).

Whereas calcification is clearly decreasing with decreasing Ω_{arag}, *P. astreoides* at Puerto Morelos are maintaining net calcification even in undersaturated seawater. These findings are similar to those of Rodolfo-Metalpa et al. (2011) (39) at Ischia, Italy, in which gross calcification occurred in transplanted subtidal calcifiers even in waters with a pH below 7.4. Additionally, other recent studies on *Porites* spp. indicate that some corals show limited, if any, negative responses to increased pCO_2 (40, 41). Physiological mechanisms that enable certain coral species to calcify under extreme levels of acidification have been suggested previously (36). It is possible, for instance, that in response to the harsher environment encountered at the springs, the corals in low or undersaturated waters use more energy to maintain their linear extension rates, but at the cost of skeletal density. This "stretch modulation" has been observed in massive *Montastrea* colonies in the Gulf of Mexico (42, 43). These observations fit well with our data, in which density decreases while linear extension rates are maintained. It has also been suggested that tissue thickness may be linked to linear extension, with thicker tissues leading to higher extension rates (44, 45), allowing the corals to overcome stress (i.e., thicker tissues are indicative of more stressful environments). No significant differences in tissue thickness between the ambient corals ($\Omega_{arag} > 3.5$) and the corals residing close to the springs ($\Omega_{arag} < 1.0$; $1 < \Omega_{arag} < 2$) were found ($P = 0.36$, Fig. 2*G*). It is interesting to note, however, that for $1.0 < \Omega_{arag} < 2.0$, a (nonsignificant) trend is seen where tissue thickness increases slightly, from an average of 3.2 mm to 3.9 mm [ANOVA $F(2,10) = 1.921$, $P = 0.19$]. This may indicate that the low saturation corals are working harder to maintain their rates of linear extension. Indeed, the extension data suggest that no significant differences are found between the low saturation and ambient corals, although a (nonsignificant) decrease in extension is observed for the corals growing in undersaturation conditions). Combined, these lines of evidence are indicative of a threshold response seen when waters reach saturation levels of ∼1.0. Above this saturation index, *P. astreoides* appear to maintain rates of linear extension by increasing their tissue thickness and compensating for decreases in pH. However, once undersaturation is reached, the energy requirements of extension appear too great for tissue thickness alone to maintain it, and a significant reduction in calcification rates is observed.

Whereas our data suggest that certain corals may be able to maintain their linear extension under the ocean acidification conditions expected by the year 2100, when considering the impact of density on bioerosion the situation is disheartening. The extent of erosion and predation by boring organisms was found to be significantly greater in corals where $\Omega_{arag} < 2.0$ ($P = 0.01$, Fig. 4). In the vicinity of the discharge, total volume eroded was 78% greater than at ambient conditions. The observed increase in total volume eroded at low saturation ($\Omega_{arag} < 2$), which is likely caused by the lower carbonate density, indicates that future acidification events may not only decrease calcification rates, but reduce coral coverage via boring organisms and mechanical erosion. For instance, it has been shown that parrotfish preferentially remove carbonates from lower density substrates (46), and the low structural integrity caused by a reduction in density could leave reefs more vulnerable to wave action, leading to a weaker framework and the further degradation of coral reefs.

Notably, our study indicates that despite their life-long exposure to low saturation waters, *P. astreoides* coral colonies at Puerto Morelos calcify at lower rates than conspecifics residing in ambient waters. These lower calcification rates are similar to those observed in short-term exposure experiments (31–33) (Fig. 3), which suggests the corals have not acclimatized to a degree that would enable the corals to maintain ambient calcification rates. Moreover, whereas some coral species are able to survive and grow in extreme conditions of undersaturation, a decrease in skeletal density combined with an increase in susceptibility to bioerosion may indicate a weakening of the reef framework in the future and subsequent degradation of the complex coral reef ecosystem.

Downloaded from https://www.pnas.org by 124.148.102.239 on April 12, 2022 from IP address 124.148.102.239.

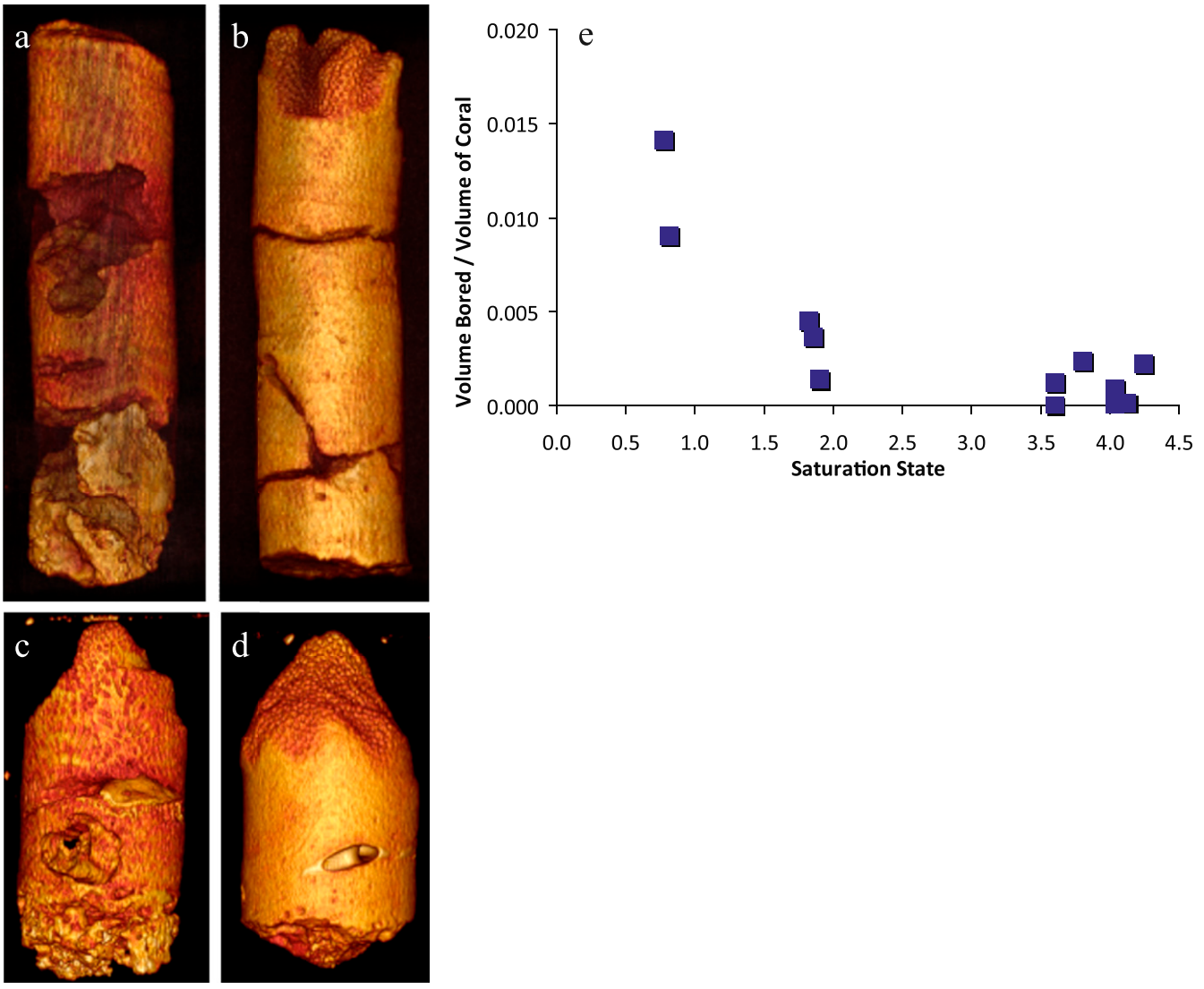

Fig. 4. Impact of Ω_{arag} on erosion and predation. The extent of erosion and predation by boring organisms was determined using the scanned images (shown as reconstructed cores of four corals). *A* and *B* are of equal size (15 cm) as are *C* and *D* (5.5 cm). The two cores from the center of a spring (*A* and *C*) are shown alongside their counterparts from ambient waters (*B* and *D*). The volume bored (normalized to the size of the core) increased by 78% with decreasing saturation state (*E*, $P = 0.01$).

Methods

The skeletal coral cores were removed from each colony with a submersible hydraulic drill, and care was taken to fill the drilled holes with cement plugs to promote tissue growth over the scar. After drying in a 50 °C oven for 5 d, the cores were scanned with a Siemens Volume Zoom spiral computerized tomography (CT) scanner at 1- to 2-mm resolution (Fig. 1). The 3D imaging capabilities of the CT scanner and software allow precise measurement of annual growth bands and a more accurate identification of the vertical growth axis than conventional X-ray techniques (20, 30). The density ($g \cdot cm^{-3}$) of each of the cores was determined using the scanned grayscale images and a conversion to apparent absolute density using pristine coral standards. Nine coral standards were used, the volume and weights of these pristine corals (no tissue no boring) were precisely measured (to the nearest 0.0001 $g \cdot cm^{-3}$) to obtain independent and precise measurements of skeletal density. These standards were scanned with the coral samples to produce a linear standard curve with densities ranging from 0.8095 to 1.5374 $g \cdot cm^{-3}$. Annual linear extension rates ($cm \cdot y^{-1}$) were obtained by precise measurement of the distance between high density bands representing annual accumulation to 0.5-mm accuracy (Fig. 1). Annual calcification rates were calculated as the product of density and linear extension (30).

The scanned images were also used to determine the extent of boring (percent volume bored) in each of the cores. Because the scanned CT images can be rotated in 3D and visualized in multiple layers, precise measurements of length, width, and depth of each bore hole can be made. The bored volume was calculated and a ratio to total coral volume was determined. To determine tissue thickness, dried cores were spliced in half and imaged using a Nikon SMZ1500 stereo microscope and SPOT imaging software. Nine measurements of tissue thickness were made per sample for statistical analysis.

Chemical analyses of the water samples were completed following those in ref. 26. From these components, the pH and saturation state were calculated using the program CO_2 Sys (47). Saturation values represent site-specific averages determined from this sampling and data reported in refs. 26 and 28.

ACKNOWLEDGMENTS. We thank G. P. Lohmann (Woods Hole Oceanographic Institution; WHOI) for help in the field and for extracting the cores, K. Rose (WHOI) for help with scanning the cores and image software analysis, Thomas DeCarlo (WHOI) for constructing the standard curve for the CT-scanned images, M. Clapham (University of California, Santa Cruz, UCSC) for help with statistical analyses, and R. Franks (UCSC) for technical assistance in the laboratory. CT scanning and coral image analyses, as well as tissue layer measurements, were conducted at WHOI. This research was funded by National Science Foundation (NSF) OCE-1040952, a University of California Institute for Mexico and the United States (UC-Mexus) grant (to A.P.), and NSF OCE-1041106 (to A.L.C.). E.D.C. was funded through NSF-GFR and a EPA-STAR fellowships. All corals were collected under Secretaría de Agricultura, Ganadería, Desarrollo Rural, Pesca y Alimentación (SAGARPA) Permit DGOPA.00153.170111.-0051 and exported with a Convention on International Trade in Endangered Species (CITES) Permit MX52912.

Downloaded from https://www.pnas.org by 124.148.102.239 on April 12, 2022 from IP address 124.148.102.239.

1. Hoegh-Guldberg O, et al. (2007) Coral reefs under rapid climate change and ocean acidification. *Science* 318(5857):1737–1742.
2. Hughes TP, et al. (2003) Climate change, human impacts, and the resilience of coral reefs. *Science* 301(5635):929–933.
3. Carpenter KE, et al. (2008) One-third of reef-building corals face elevated extinction risk from climate change and local impacts. *Science* 321(5888):560–563.
4. Barbier EB, et al. (2011) The value of estuarine and coastal ecosystems. *Ecol Monogr* 81:169–193.
5. Fabry VJ, Seibel BA, Feely RA, Orr JC (2008) Impacts of ocean acidification on marine fauna and ecosystem processes. *ICES J Mar Sci* 65(3):414–432.
6. Caldeira K, Wickett M (2005) Ocean model predictions of chemistry changes from carbon dioxide emissions to the atmosphere and ocean. *J Geophys Res* 110:C09S04.
7. Orr JC, et al. (2005) Anthropogenic ocean acidification over the twenty-first century and its impact on calcifying organisms. *Nature* 437(7059):681–686.
8. Doney SC, Fabry VJ, Feely RA, Kleypas JA (2009) Ocean acidification: The other CO_2 problem. *Annu Rev Mar Sci* 1:169–192.
9. Feely RA, Doney SC, Cooley SR (2009) Ocean acidification: Present conditions and future changes in a high CO_2 world. *Oceanography (Wash DC)* 22:36–47.
10. Cao L, Caldeira K (2008) Atmospheric CO2 stabilization and ocean acidification. *Geophys Res Lett* 35(19):L19609, 10.1029/2008GL035072.
11. Langdon C, Atkinson MJ (2005) Effect of elevated pCO_2 on photosynthesis and calcification of corals and interactions with seasonal change in temperature/ irradiance and nutrient enrichment. *J Geophys Res* 110:C09S07, 10.1029/2004JC002576.
12. Caldeira K, Wickett ME (2003) Oceanography: Anthropogenic carbon and ocean pH. *Nature* 425(6956):365–377.
13. Gattuso JP, Frankignoulle M, Bourge I, Romaine S, Buddemeier RW (1998) Effect of calcium carbonate saturation of seawater on coral calcification. *Global Planet Change* 18:37–46.
14. Leclercq N, Gattuso JP, Jaubert J (2002) Primary production, respiration, and calcification of a coral reef mesocosm under increased CO2 partial pressure. *Limnol Oceanogr* 47:558–564.
15. Jokiel PL, et al. (2008) Ocean acidification and calcifying reef organisms: A mesocosm investigation. *Coral Reefs* 27:473–483.
16. Schneider K, Erez J (2006) The effect of carbonate chemistry on calcification and photosynthesis in the hermatypic coral *Acropora eurystoma*. *Limnol Oceanogr* 51:1284–1295.
17. Pandolfi JM, Connolly SR, Marshall DJ, Cohen AL (2011) Projecting coral reef futures under global warming and ocean acidification. *Science* 333(6041):418–422.
18. Fabricius KE, et al. (2011) Losers and winners in coral reefs acclimatized to elevated carbon dioxide concentrations. *Nature Climate Change* 1:165–169.
19. Cooper TF, De'ath G, Fabricius KE, Lough JM (2008) Declining coral calcification in massive Porites in two nearshore regions of the Great Barrier Reef. *Glob Change Biol* 14:529–538.
20. De'ath G, Lough JM, Fabricius KE (2009) Declining coral calcification on the Great Barrier Reef. *Science* 323(5910):116–119.
21. Tanzil JTI, Brown BE, Tudhope AW, Dunne RP (2009) Decline in skeletal growth of the coral Porites lutea from the Andaman Sea, South Thailand between 1984 and 2005. *Coral Reefs* 28(2):519–528.
22. Hoegh-Guldberg O, Ortiz JC, Dove S (2011) The future of coral reefs. *Science* 334(6062):1494–1495, author reply 1495–1496.
23. Pandolfi JM, Connolly SR, Marshall DJ, Cohen AL (2011) Response. *Science* 334: 1495–1496.
24. Medina-Elizalde M, Rohling EJ (2012) Collapse of Classic Maya civilization related to modest reduction in precipitation. *Science* 335(6071):956–959.
25. Beddows PA, Smart PL, Whitaker FF, Smith SL (2007) Decoupled fresh-saline groundwater circulation of a coastal carbonate aquifer: Spatial patterns of temperature and specific electrical conductivity. *J Hydrol (Amst)* 246:18–32.
26. Crook ED, Potts D, Rebolledo-Vieyra M, Hernandez L, Paytan A (2011) Calcifying coral abundance near low pH springs: Implications for future ocean acidification. *Coral Reefs* 31(1):239–245.
27. Inoue M, et al. (2012) Estimate of calcification responses to thermal and freshening stresses based on culture experiments with symbiotic and aposymbiotic primary polyps of a coral, Acropora digitifera. *Global Planet Change* 92–93:1–7.
28. Hofmann GE, et al. (2011) High-frequency dynamics of ocean pH: A multi-ecosystem comparison. *PLoS ONE* 6(12):e28983, 10.1371/journal.pone.0028983.
29. Saenger C, Cohen AL, Oppo DW, Halley RB, Carilli JE (2009) Surface-temperature trends and variability in the low-latitude North Atlantic since 1552. *Nat Geosci* 2:492–495.
30. Cantin NE, Cohen AL, Karnauskas KB, Tarrant AM, McCorkle DC (2010) Ocean warming slows coral growth in the central Red Sea. *Science* 329(5989):322–325.
31. de Putron SJ, McCorkle DC, Cohen AL, Dillon AB (2011) The impact of seawater saturation state and bicarbonate ion concentration on calcification by new recruits of two Atlantic corals. *Coral Reefs* 30:321–328.
32. Albright R, Langdon C (2011) Ocean acidification impacts multiple early life history processes of the Caribbean coral Porites astreoides. *Glob Change Biol* 17:2478–2487.
33. Anthony KRN, Kline DI, Diaz-Pulido G, Dove S, Hoegh-Guldberg O (2008) Ocean acidification causes bleaching and productivity loss in coral reef builders. *Proc Natl Acad Sci USA* 105(45):17442–17446.
34. Kleypas JA, et al. (1999) Geochemical consequences of increased atmospheric carbon dioxide on coral reefs. *Science* 284(5411):118–120.
35. Leclercq N, Gattuso JP, Jaubert J (2000) CO_2 partial pressure controls the calcification rate of a coral community. *Glob Change Biol* 6:329–334.
36. Cohen AL, Holcomb M (2009) Why corals care about ocean acidification: Uncovering the mechanism. *Oceanography (Wash DC)* 22:118–127.
37. Ries JB, Cohen AL, McCorkle DC (2009) Marine calcifiers exhibit mixed responses to CO_2 induced ocean acidification. *Geology* 37:1131–1134.
38. Holcomb MC, McCorkle DC, Cohen AL (2009) Long-term effects of nutrient and CO_2 enrichment on the temperate coral *Astrangia poculata* (Ellis and Solander, 1786). *J Exp Mar Biol Ecol* 386:27–33.
39. Rodolfo-Metalpa R, et al. (2011) Coral and mollusc resistance to ocean acidification adversely affected by warming. *Nature Climate Change* 1:308–312.
40. Edmunds PJ, Brown D, Moriarty V (2012) Interactive effects of ocean acidification and temperature on two scleractinian corals from Moorea, French Polynesia. *Glob Change Biol* 18:2173–2183, 10.1111/j.1365-2486.2012.02695.x.
41. Comeau S, Edmunds PJ, Spindel NB, Carpenter RC (2013) The responses of eight coral reef calcifiers to increasing partial pressure of CO2 do not exhibit a tipping point. *Limnol Oceanogr* 58:388–398, 10.4319/lo.2013.58.1.0388.
42. Carricart-Ganivet JP, Merino M (2001) Growth responses of the reef-building coral *Montastraea annularis* along a gradient of continental influence in the southern Gulf of Mexico. *Bull Mar Sci* 68:133–146.
43. Carricart-Ganivet JP (2004) Sea surface temperature and the growth of the West Atlantic reef-building coral *Montastraea annularis*. *J Exp Mar Biol Ecol* 302:249–260.
44. Lough JM, Barnes DJ (2000) Environmental controls on growth of the massive coral *Porites*. *J Exp Mar Biol Ecol* 245(2):225–243.
45. Barnes DJ, Lough JM (1992) Systematic variations in the depth of skeleton occupied by coral tissue in massive colonies of *Porites* from the Great Barrier Reef. *J Exp Mar Biol Ecol* 159:113–128.
46. Bruggemann H, van Kessel AM, van Rooij JM, Breeman AM (1996) Bioerosion and sediment ingestion by the Caribbean parrotfish *Scarus vetula* and *Sparisoma viride:* Implications of fish size, feeding mode and habitat use. *Mar Ecol Prog Ser* 134:59–71.
47. Pierrot D, Lewis E, Wallace DWR (2006) MS Excel Program Developed for CO2 System Calculations. ORNL/CDIAC-105a Carbon Dioxide Information Analysis Center, Oak Ridge National Laboratory (US Department of Energy, Washington, DC).

Downloaded from https://www.pnas.org by 124.148.102.239 on April 12, 2022 from IP address 124.148.102.239.